

Received 28 February 2023, accepted 14 March 2023, date of publication 23 March 2023, date of current version 6 April 2023.

Digital Object Identifier 10.1109/ACCESS.2023.3260622

SURVEY

An Efficient Coverage Area Re-Assignment Strategy for Multi-Robot Long-Term Surveillance

SEUNGHWAN LEE¹, (Member, IEEE)

School of Electronic Engineering, Kumoh National Institute of Technology, Gumi 39177, Republic of Korea

e-mail: leesh@kumoh.ac.kr

This work was supported in part by the Project titled “Research on Co-Operative Mobile Robot System Technology for Polar Region Development and Exploration” funded by the Korean Ministry of Trade, Industry and Energy under Grant 1525011633; in part by the LG Electronics; and in part by the Government-Wide Research and Development Fund for Infections Disease Research (GFID) funded by the Ministry of the Interior and Safety, Republic of Korea, under Grant 20014854.

ABSTRACT This study deals with a new strategy of the re-assignment for multi-robot seamless coverage tasks using the concept of propagation in a multi-robot surveillance system (MRSS). In the context of MRSSs, multi-robot coverage tasks play a critical role. These tasks require generating paths for two or more robots to cover an entire area, with the objective of minimizing the time needed to complete the task. However, over time, robots may need to be excluded from coverage missions due to issues such as battery charging or malfunctions. It is important to handle these situations efficiently in order to maintain the completeness and balance of the coverage mission. Typically, it can be resolved by either recomputing the coverage algorithm for the remaining robots or redistributing the coverage task of the excluded robot to its neighbors. However, in the proposed method, the amount of coverage area of the excluded robot is equally and efficiently assigned to the remaining robots. First off, a relational graph between robots and a tree based on the excluded robot are sequentially constructed to necessarily know how the robots are geometrically arranged in the given area centered on the excluded robot. The excluded robot becomes the root of the tree, and the depth of the tree indicates the proximity of the coverage areas. Subsequently, the amount of the original coverage area of the excluded robot can be differently assigned to its nearest neighbor robots according to the size of the subtree. Then, the coverage area of the robots corresponding to the second level of the tree are added from the partial coverage area of their parent robot to keep their coverage area balanced, respectively. The similar process is continuously performed, such as ‘propagation’, until the re-assignment of the coverage area over the leaf nodes is complete. Finally, balanced coverage area is re-assigned to the remaining robots, which is time-efficiently computed. Simulations were performed on two occupancy grid maps that were acquired from a simultaneous localization and mapping method. The proposed method was evaluated against conventional methods on three factors such as the balanced re-assignment of the coverage area (*Balancing*), the variation of the individual coverage area before and after the re-assignment process (*Seamless Coverage*), and the total computational efficiency over time (*Time-efficiency*). The coverage area was uniformly re-allocated after the proposed method was applied. In addition, the proposed method had a short calculation time and enables seamless coverage even after re-allocation. In the future, probabilistic maps related to the importance rate, accident rate, and crowds in the coverage area will also be taken into consideration.

INDEX TERMS Multi-robot coverage task, multi-robot coverage path re-planning, multi-robot surveillance system.

I. INTRODUCTION

With the increase in unmanned surveillance systems, the necessity of using multiple robots has increased [1], [2],

The associate editor coordinating the review of this manuscript and approving it for publication was Maged Abdullah Esmail¹.

[3], [4], [5]. The essence of the multi-robot surveillance system (MRSS) is for multiple robots to completely cover a given area within a limited time. This can be called multi-robot coverage path planning (MCP) in the MRSS [6]. MCP is a special case of coverage path planning (CPP) that involves generating a path for a robot or multiple

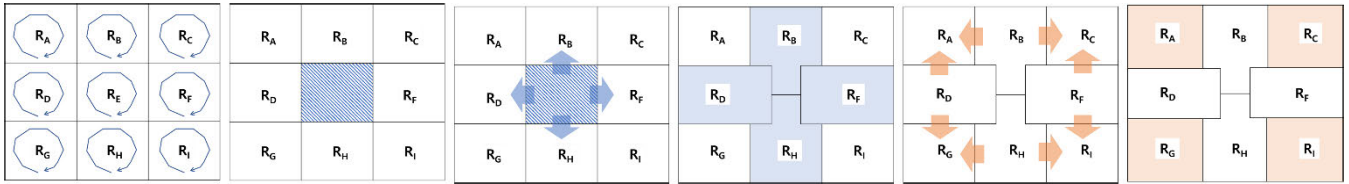


FIGURE 1. Illustration of necessity of the proposed approach in a scenario. Nine robots cover different areas in a designated area simultaneously. If a robot, R_F , is excluded from the robot team due to battery charging, its coverage area is no longer monitored. To ensure seamless coverage, the area can be assigned to the nearest neighboring robots. Alternatively, the viewpoints of the eight remaining robots can be intuitively recalculated and reassigned. However, these methods cannot uniformly and efficiently redistribute R_F 's coverage area to the other robots in the team. This study proposes a detailed area propagation method to cope with this issue.

robots that covers the entire area while minimizing the time required to complete the coverage task [7]. CPP differs from general path planning [8] in that it focuses on area coverage, rather than just finding a path between a starting and goal point.

MCPM of the surveillance system [9] is more complex than that of the general cleaning system [10]. Unlike a typical cleaning robot system that only considers visited points, the surveillance system must take into account both the viewpoints of the robots and the sensing area detected by their sensors at each corresponding point. To carry out a robot patrolling mission in a multi-robot surveillance system for an extended period, it is crucial to devise countermeasures against deviations from the coverage mission due to robot battery charging or malfunction. This is one of the most significant and practical challenges that must be addressed for the long-term operation of surveillance systems.

Fig. 1 depicts a description of the balanced and efficient re-allocation for the required coverage area. In this scenario, nine robots were represented that initially covered a designated area [3]. When a robot, R_F , is excluded from the robot team because of battery charging, its coverage area is no longer monitored. However, the task of covering the area can be assigned to the nearest neighbors of R_F , thus enabling complete recovery of the coverage [11]. Alternatively, the viewpoints of the eight robots over the entire area can be recomputed and reassigned. However, this approach allocates new coverage areas to the remaining robots in a unilateral manner, which can lead to confusion in the entire coverage task and even cause collision problems during transit to new coverage areas. To mitigate these issues, a form of area propagation can be envisioned, which is thoroughly proposed in this study. The main contributions of this study are as follows:

1. To achieve complete coverage, a robot relational graph and a tree structure are constructed when a robot is excluded from the coverage mission.

2. A propagation-based coverage area re-allocation method has been proposed using the level of the tree structure. This method has three advantages: equal distribution of coverage areas, minimization of changes to the original coverage tasks, and high time efficiency.

3. In the performance comparison, all approaches are evaluated based on three factors: the balance of the coverage area re-assignment, the variation of the individual coverage

area before and after the re-assignment process, and the overall computational time.

II. RELATED WORK

Comprehensive studies on CPP for a single robot have been conducted [12], [13]. Their field of research was mainly concerned with coverage completeness and minimizing overlap of coverage paths [14]. Furthermore, these studies were carried out for various applications such as disinfecting robots [15], harvesting robots [16], vacuum cleaning robots [17], and surveillance robots [3].

In CPP, MCPM is considered a challenge [18]. However, compared to single-robot CPP, MCPM has several advantages, including reduced time consumption and improved execution efficiency by completing tasks in parallel [6]. In addition, if some members of the robot team fail, other robots can compensate for the problem [13], which improves the system's robustness.

MCPM is the process by which a robotics team computes a set of actionable paths that encapsulates a set of viewpoints that must be visited, each with an assigned path, in order to completely scan, navigate, or investigate the structure or environment of interest [7]. In [19], MCPM algorithms were compared. There are two types of approaches: the multi-level subgraph patrolling (MSP) algorithm [20] and cyclic coverage. The MSP algorithm is a multi-step segmentation algorithm that assigns different regions (subgraphs) to each mobile agent. This algorithm effectively computes the path of any robot using the classical algorithm for Euler cycles and various heuristics for Hamilton cycles, non-Hamilton cycles, and the longest paths. The algorithm was compared to the cyclic algorithm presented in [21]. The MSP algorithm performed slightly better in half of the cases and slightly worse in the other half.

Several studies [22], [23], [24] have considered the use of multiple unmanned aerial vehicles (UAVs) for MCPM. The aim of these studies was to improve the efficiency of MCPM itself for UAVs with varying capabilities by using clustering or optimization algorithms, such as the ant colony algorithm. However, these research works did not deeply consider resilience scenarios involving faults or charging requirements.

In MRSSs, MCPM studies are broadly categorized into distributed and centralized methods. One of distributed methods was proposed in [25] for increasing the speed

of exploration work through multi-robot cooperation. This method used an auction-based approach to handle broken robots and assigned new tasks to the remaining robots based on their bids. However, a drawback of this method is that it can be challenging to ensure area balancing and seamless coverage because it may be difficult to consider the entire situation. Centralized patrolling methods that use graph theory are sub-divided into two categories [26], which are cyclic [27] and graph partitioning methods [28]. In cyclic methods, robots follow a predefined cyclic path across all vertices in the graph and this path is computed as a solution to the traveling salesman problem (TSP) which is a known NP-hard problem. In graph partitioning methods, the map is partitioned into different disjoint regions, and each region is assigned to a robot for patrolling the region independently.

In MRSSs, MCPP includes an additional constraint according to the sensing range of the equipped sensors on each robot [29], [30]. This is because not only the viewpoints that the robot should visit but also the area detected around them can be considered covered. In particular, in [29], an area consisting of obstacles with polygonal shapes was covered using cluster-based algorithms and a cyclic coverage method. Viewpoints were generated according to the trapezoidation process using a limited visual range.

The concept of resilience was partially discussed in [11] and [31]. Especially, in [32], a distributed method called cooperative autonomy for resilience and efficiency was proposed. It not only provided resilience to the robot team against failures of individual robots but also improved operational efficiency with event-based re-planning. In particular, the game-theoretic structure built using Potential Games [33] considers only the nearest neighbors of the failed robot in a resilience game. In this study, because the balanced re-assignment of the coverage area is one of the most important criteria, performance comparisons with the above method are also considered.

Initially, the problem of the surveillance system was defined as the Art Gallery Problem (AGP), which was a well-known problem formulated by Klee in [34]. This problem can be solved by determining the minimum number of guards required to cover the entire gallery, which has also been considered in 3D [35]. These works considered several static sensors as guards, which can be applied to closed-circuit television (CCTV) surveillance systems.

One graph-based coverage approach [29] utilizes the concept of AGP to consider the sensing range in MCPP. The first step is to generate a uniform set of points called static guards so that the entire area of interest (AOI) can be observed. The robots participating in the coverage mission must then visit the points to cover the AOI. The second step involves creating a graph that connects the guard and workspace nodes. The third and fourth steps are to reduce the size of the graph and use multiple robots to cover the graph, respectively. However, the gaps between the generated viewpoints were not constant, and the fault tolerance of some robots in the long term was not considered.

In [3], the work introduced in [29] and [30] was improved and extended to MCPP. The viewpoints were extracted based on the normal vectors of the occupied points in the given map. To balance the number of viewpoints, several heuristic parts, such as the path division and recombination parts, were considered. In this study, initial MCPP was performed in a similar manner. In a study [36], the problem of unbalanced multi-robot coverage was addressed using Voronoi partitioning. The study showed an improvement in terms of workload balance among the robots compared to the KH algorithm.

To solve the MCPP problem, research has been conducted from the viewpoint of cooperative exploration [37] or different velocities [38]. In [39], when a graph-based representation of the occupancy grid map is given, an edge probability heat graph is constructed using a CNN, which can obtain near-optimal solutions of the CPP. For complete coverage [40], an energy-aware back-and-forth coverage path planning approach is required. They considered the best configuration of back-and-forth motions at the maximum altitude in resolution constraints while minimizing the number of turns [41]. However, there have been few studies that can effectively reassign the coverage area when a robot fails, or the battery needs to be charged.

III. PROPOSED APPROACH

In this study, the proposed method ensures that the remaining robots do not have any problems with the overall coverage mission, even if a robot conducting the coverage deviates from the robot team owing to battery charging or fault. To make this possible, a propagation concept is adopted. This is based on the phenomenon of radio waves in nature and involves sequentially reallocating the coverage areas of an excluded robot, starting from those that are at the periphery. As a result, the coverage area of the excluded robot is uniformly distributed to the coverage loads of the remaining robots. The proposed method consists of four processes as shown in Fig. 2. First off, a relational graph between the robots was constructed. Based on this graph, a tree was configured from the excluded robot. Subsequently, the coverage area was re-allocated via the propagation scheme, which is the core of the proposed approach. Finally, the coverage paths of the remaining robots were re-planned using the updated coverage area.

The coverage areas and paths of multiple robots were initially assigned and generated according to the method presented in [3]. In this process, the sensing range of each robot, named S_r , is considered as the spacing of the nodes that the robots should visit for full coverage. Because the proposed method can be operated depending on the existence of a robot excluded from the coverage mission, it is assumed that the situation has occurred in the description below.

A. CONSTRUCTION OF ROBOT RELATIONAL GRAPH

In initial MCPP, a graph of the road map of the i -th robot was constructed in advance, which is named G_i^j . It includes nodes,

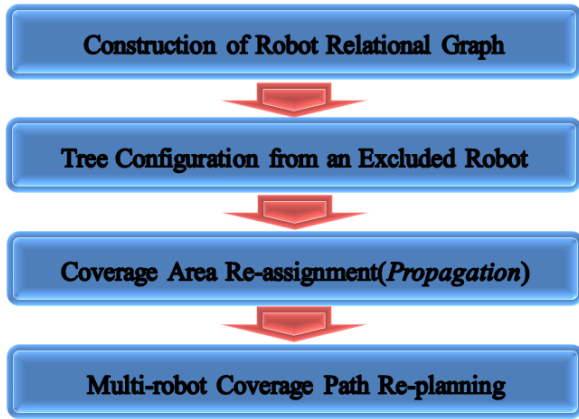


FIGURE 2. Overall structure of the proposed method. It has four steps such as the construction of a robot relational graph, tree configuration from an excluded robot and coverage area re-allocation, the core of the proposed approach, i.e., *Propagation*, coverage path re-planning of the individual robots from the updated their own coverage area.

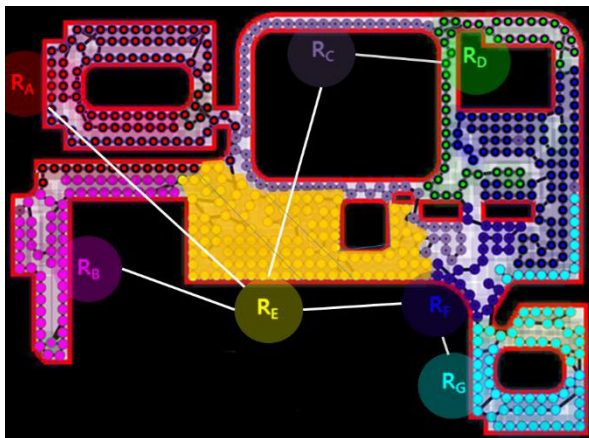


FIGURE 3. An illustration of multi-robot coverage. In this example, the initial coverage areas of seven robots such as R_A , R_B , R_C , R_D , R_E , R_F and R_G are assigned on the map. The coverage area of R_E with yellow color will be re-assigned.

V_p^i , and edges, E_p^i , regarding the movement of the robots. However, in order to re-assign the coverage area of a robot that has departed from the coverage mission to the remaining robots, proximity between robots is essential. To represent this, a robot relational graph, named G_r , is constructed, which is based on the geometric coverage area of robots. G_r consists of V_r and E_r which denote nodes describing the remaining robots themselves and edges indicating whether or not nodes are adjacent as follows.

$$E_r(i, j) = \begin{cases} 1, & \text{if } Dist(V_r(i), V_r(j)) \leq S_r + \delta \\ 0, & \text{otherwise} \end{cases} \quad (1)$$

where $Dist(V_r(i), V_r(j))$ represents the minimum distance between V_p^i and V_p^j . If the distance is less than or equal to $S_r + \delta$, then, $V_r(i)$ and $V_r(j)$ are *adjacent*. ‘adjacent’ indicates their coverage areas are adjacent.

For example, suppose that the coverage areas of the seven patrolling robots are initially assigned on the map as shown in Fig. 3. To construct a graph G_r for the seven robots R_A , R_B , R_C , R_D , R_E , R_F , and R_G , their connectivity is determined

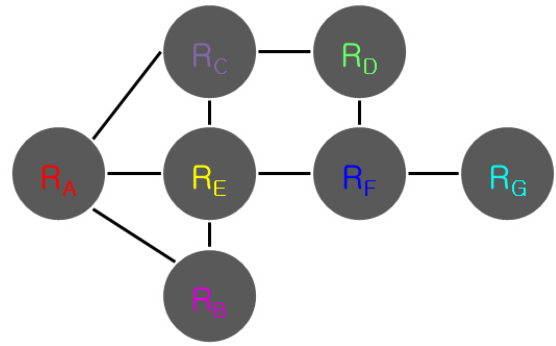


FIGURE 4. Example of a robot relational graph, G_r . Robots adjacent to robot R_A were R_B , R_C , and R_E . In addition, robots adjacent to R_C were R_A and R_D . R_F had an adjacent relationship with R_E , R_D , and R_G .

based on (1). In the graph, the robots correspond to $V_r(1)$, $V_r(2)$, ..., and $V_r(7)$, respectively.

The result is shown in Fig. 4. The robots adjacent to robot R_A are R_B , R_C , and R_E . In addition, robots adjacent to R_C are R_A and R_D . R_F has an adjacent relationship with R_E , R_D , and R_G .

The structure of the graph indicates the density of the coverage areas of the robots in the entire area.

B. TREE CONFIGURATION FROM THE EXCLUDED ROBOT

In a long-term operation in a MRSS, any robot can be excluded from the coverage mission owing to battery charging or its faults, as mentioned previously. To cope with this, a tree, T , for appropriate re-assignment of the entire coverage area is constructed using G_r . The root of T represents an excluded robot. In this example, it is assumed that the battery of R_E drops below a certain level. Subsequently, T can be constructed as shown in Fig. 4. As R_A , R_B , R_C , and R_F are known to be adjacent to the R_E from G_r , they constitute the 1st level of T . In addition, R_D and R_G closest to the R_F are configured as nodes for the 2nd level of T . In the case of R_D , because it is closest to R_C , it may also be a child node of R_C once T is configured. This is determined by the order of execution during the construction of T .

C. PROPAGATION

The coverage area of the excluded robot that needs to be reassigned must be equally divided among the remaining robots. In addition, the split coverage area was added to each robot to minimize its impact on the ongoing coverage mission. This section explains the concept of propagation using the levels of T .

First off, it is necessary to uniformly re-assign the coverage area of the excluded robot, which is the root node of the tree, to surrounding robots. Neighbor robots of the excluded robot are robots with the child nodes of the root node, which is said to be the 1st level of nodes in T . The coverage area of the excluded robot was divided and assigned to the robots corresponding to the 1st level of the nodes. In the example, if the size of the coverage area of the R_E is 100, the area is intuitively allocated to robots of the first level in T by

25% of the area because the number of first-level nodes, *i.e.*, R_A , R_B , R_C , and R_F is four. This approach is similar to that suggested in [32]. However, in that case, the coverage areas of R_D and R_G corresponding to the 2nd level are maintained as they are, resulting in only the robots corresponding to the 1st level increase their coverage area. This is expected to show poor performance in terms of the *minimum worst visiting period* which is one of the ultimate goals for an optimal patrol in the surveillance system. In other words, because the number of robots has changed from seven to six owing to the excluded robot, The best solution in terms of the balanced re-assignment of the coverage area is to divide the coverage area of the excluded robot by a percentage of 16.7 and assign it to each robot's coverage area. In this study, a matrix representing the coverage assignment quantity was defined to properly allocate the coverage area of the excluded robot according to the level and size of the tree structure. The matrix is represented as $M_L(i, j)$, as listed in Table 1.

TABLE 1. Matrix M_L for the re-allocation amount by level of the tree in the example.

1	0	0	0	0	0	0	0
1	0	0	0	0	0	0	0
1	0	0	0	0	0	0	0
0	1	0	0	0	0	0	0
0	0	0	0	0	0	0	0
3	0	0	0	0	0	0	0
0	1	0	0	0	0	0	0

The i -th row of M_L denotes the order of the robots and the j -th column denotes the level of the tree. In the first level, a coverage area of 1 was assigned to the R_A , R_B , and R_C because they had no children in the tree. However, because the R_F has two child nodes, the allocated coverage area is 3. Similarly, at the second level, R_D and R_G have no child nodes, and the size of the assigned coverage area is 1.

The relative coverage area to be allocated was determined using M_L . The coverage area for the excluded robot, R_E , is called A_{R_E} . This denotes a cardinality represented as $n(V_p^{R_E})$ and is re-assigned to each robot as follows:

$$A_{R_i} = \frac{M_L(i, j)}{N_R - 1} A_{R_E}, \text{ for all } i \quad (2)$$

where A_{R_i} is the additional coverage area of R_i after re-allocation. j is determined by the level of R_i in tree. N_R denotes the number of robots used. Because A_{R_E} is 100 and N_R is 6, $V_p^{R_E}$ is divided into six equal parts. In the case of R_A , R_B , and R_C , because the elements of M_L regarding them are filled with 1, only 16.7 percent of $V_p^{R_E}$ is additionally allocated. However, because the relative amount of coverage area in R_F is three, the size of the additional coverage area for R_F is half that of A_{R_E} .

Now, we consider the second level of T . At the second level, the relative coverage sizes of both R_D and R_G were 1.

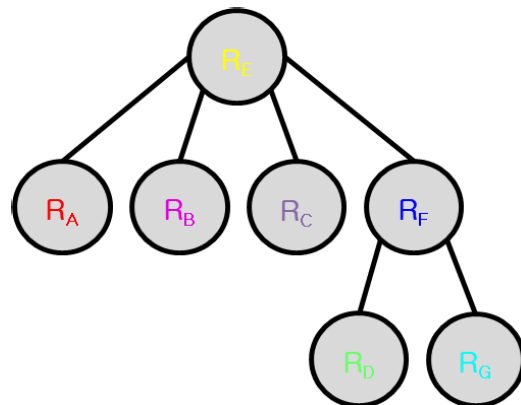
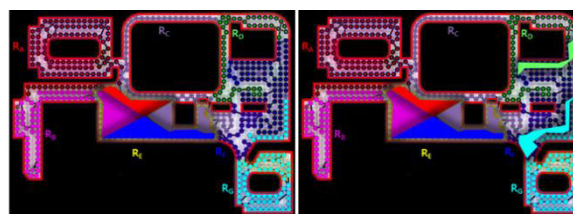


FIGURE 5. Tree structure for the re-assignment of the coverage area of R_E . The root node of the tree is R_E . R_A , R_B , R_C , and R_F make up the first level of the tree. The second level of the tree that is the same as the leaf node of the tree indicates R_D and R_G .



(a) The 1st level of the tree (b) The 2nd level of the tree

FIGURE 6. Expected coverage area re-assignment results according to the level of the tree in the example.

Since they are connected to the R_F in T , the coverage area close to R_D and R_G among the entire coverage areas of the R_F should be added to each coverage area. This is a form of taking part in the R_F coverage area. This is illustrated in Fig. 6.

R_F obtains three times more area than any other robot in the vicinity and re-allocates two-thirds of the allocated amount to R_D and R_G , respectively. This process ensures that the entire coverage area is uniformly distributed, and the ongoing patrol missions of the individual robots are also minimally affected. When R_E is excluded from the coverage mission, if the entire area is newly allocated to the remaining robots, it will bring a significant change to coverage area of each robot. However, the proposed propagation scheme minimizes changes in each coverage area and simultaneously attempts to distribute the coverage area of the R_E equally.

The proposed algorithm can be iteratively performed in the same manner if there are additional levels, such as the third and fourth levels in the tree. Although the amount of coverage area to be allocated is determined, it is not specified which nodes involved in the coverage area will be added to one of each robot. In this study, the specific allocation process for the coverage area was divided into two parts.

In the first part, it redistributes the entire coverage area of the excluded robot to the robots corresponding to the first level of the tree according to A_{R_i} . The nodes to be assigned are selected individually in the order of the closest nodes in the border of the coverage area. However, in the coverage

area allocation process, there may be a problem in that not all nodes can be allocated according to A_{R_i} . For instance, suppose a temporary node is intended to be assigned to robot R_i to coincide with A_{R_i} , but it might be obstructed by the coverage area of another robot R_j . In such a scenario, the node will be allocated to R_j instead, and then R_i will retrieve a different node from R_j through a readjustment process.

The following is a part of the *propagation*. Because the area allocation size, A_{R_i} has already been calculated, the distance between them must be calculated to appropriately transfer the partial coverage area of a parent node of R_i in T to $V_p^{R_i}$. A number of proximity nodes are extracted based on the distance while A_{R_i} is reflected. This process is repeated until the child nodes correspond to the leaf nodes of T . Finally, each robot has its own updated coverage area for patrolling. The entire process is described in Algorithm 1. Algorithm 2 is a process in which coverage nodes are transferred between parents and children in the real tree.

Algorithm 1 Algorithm for Propagation

Input: $R_E, G_p, G_r, N_R, A_{R_E}$

N_R : number of robots

R_E : excluded robot

A_{R_E} : the size of the coverage area of the excluded robot

G_p^E : a graph of the road map of the excluded robot

Output: Updated G_p for all robots

$T \leftarrow$ Construction of Tree(R_E, G_p, G_r)

$N_T \leftarrow$ Depth of T

$M_L \leftarrow$ Construction of Coverage Re-assignment Matrix(T)

for $j = 1: N_T$

 for $i = 1: N_R$

 Compute A_{R_i} using (2)

 if $j=1$, then, (First Depth)

$G_p^i, G_p^E = \text{Region_reassignment}(R_i, R_E, A_{R_i},$

$G_p^i, G_p^E)$

 else (Second Depth, Third Depth, ...)

$R_p =$ parents of R_i in T

$G_p^i, G_p^p = \text{Region_reassignment}(R_i, R_p, A_{R_i},$

$G_p^i, G_p^p)$

 end if

 end for

end for

D. MULTI-ROBOT COVERAGE PATH RE-PLANNING

After the re-assignment of the coverage area, the individual graphs for the i -th robot G_p^i are updated. The coverage path of each robot is also re-planned, which is a well-known traveling salesman problem (TSP). The nearest neighbor based CPP is performed by selecting the minimum cost among the candidate coverage paths. Because individual coverage missions are in progress, the TSP tour is re-calculated using a starting point fixed at each robot's current location.

Algorithm 2 Algorithm for Region_reassignment

Input: $R_i, R_j, A_{R_i}, G_p^i, G_p^j$

Output: G_p^i, G_p^j

for $j = 1: A_{R_i}$

$[idx] = \text{argDist}(V_p^j, V_p^i) - \text{ascending order index}$

$G_p^i \leftarrow$ Add Node ($V_p^j(idx)$) - add by order

$E_a \leftarrow$ Generation of Additional Edges between V_p^i and $V_p^j(idx)$

$G_p^i \leftarrow$ Add Edges (E_a)

$G_p^j \leftarrow$ Delete Node ($V_p^j(idx)$) and Corresponding Edge

end for

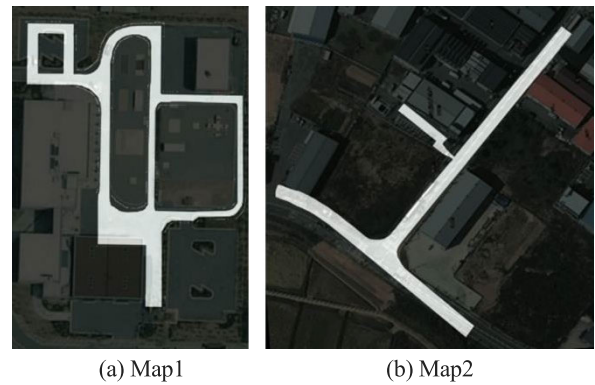


FIGURE 7. Simulation maps with Google maps. The simulation maps are obtained using SLAM method [42] in Gwangju and Pohang in Republic of Korea, respectively.

IV. SIMULATION

In the simulations, two occupancy grid maps that were initially built using a Simultaneous Localization and Mapping (SLAM) algorithm [42] were exploited and refined to operate MCPP. The maps are shown in Fig. 7. Accurate positioning and map building are important processes in practical multi-robot surveillance system. However, in this study, the re-allocation of MCPP is the main focus; thus, accurate positioning and map building are not addressed seriously.

Each robot had its own LiDAR sensor with a range S_r . In this section, the number of robots is varied in each experiment such as 2, 3, 5, and 10. In addition, S_r was changed to 10m, 25m, and 40m. In addition, the three types of factors are the balanced re-assignment of the coverage area, variation of the individual coverage area before and after the re-assignment process, and overall computational time.

A. INITIAL COVERAGE AREA ASSIGNMENT

MCPP can be performed according to [3], which generates the initial coverage paths for N_R robots with S_r . The construction results of three G_p values for different S_r are shown in Fig. 8. Dotted circles indicate lidar sensing ranges according to S_r . Their centers represent viewpoints V_p that the robots should visit.

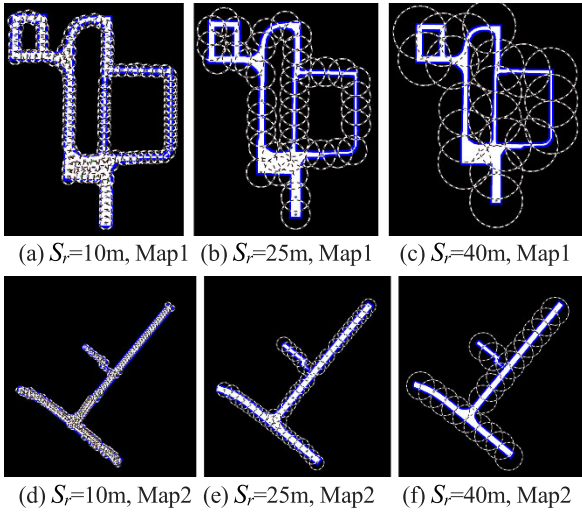


FIGURE 8. Construction results of three G_p regarding different S_r . The dotted circles indicate lidar sensing ranges according to S_r . Their centers represent viewpoints V_p that the robots should visit.

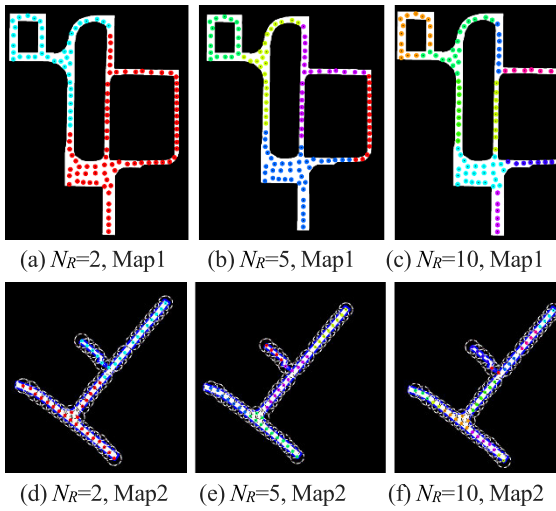


FIGURE 9. Initial coverage allocation results for N_R robots. MCPP is also computed, and multiple robots conducted their coverage tasks according to the results of MCPP.

Fig. 9 shows the initial coverage allocation results for N_R robots. The MCPP is also computed, and multiple robots conduct their coverage tasks according to the MCPP results.

B. COVERAGE AREA RE-ASSIGNMENT

When a robot is excluded from the coverage mission owing to its fault or battery charging, a re-assignment process can be conducted. The three algorithms were compared in this section. One is to re-compute the entire coverage area for N_R-1 robots following the procedures described in [3]. N_R-1 areas obtained after recalculation of the entire area were assigned to the robots with the most overlapping area with their coverage area. (additional implementation of the most overlapping area search algorithm). Another one considers only the nearest neighbor of the excluded robot which is similar to [32]. The third algorithm is the proposed propagation-based re-assignment algorithm.

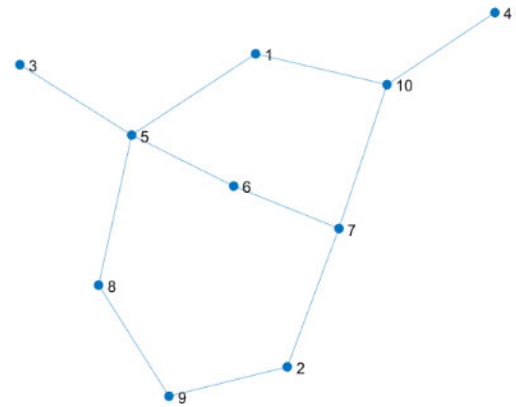


FIGURE 10. An example of G_r for $N_R = 10$. Each has neighbors adjacent to its coverage area.

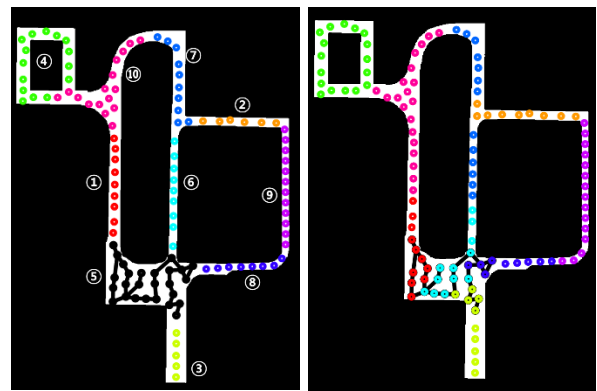


FIGURE 11. Coverage area re-assignment results according to the level of the tree in the example. The entire coverage area of R_E (black, ⑤) is assigned to 1st level (①,③,⑥,⑧) of nodes in T . Subsequently, the coverage area is propagated to robots in the remaining levels of the tree.

Fig. 10 shows an example of G_r for $N_R = 10$. Each has neighbors adjacent to its coverage area. In the simulation, it was assumed that robot R_E was excluded. In the propagation process, M_L is constructed using T as follows:

$$M_L = \begin{bmatrix} 3 & 0 & 0 & 0 & 0 & 0 & 0 & 0 & 0 & 0 \\ 0 & 0 & 1 & 0 & 0 & 0 & 0 & 0 & 0 & 0 \\ 1 & 0 & 0 & 0 & 0 & 0 & 0 & 0 & 0 & 0 \\ 0 & 0 & 1 & 0 & 0 & 0 & 0 & 0 & 0 & 0 \\ 0 & 0 & 0 & 0 & 0 & 0 & 0 & 0 & 0 & 0 \\ 3 & 0 & 0 & 0 & 0 & 0 & 0 & 0 & 0 & 0 \\ 0 & 2 & 0 & 0 & 0 & 0 & 0 & 0 & 0 & 0 \\ 2 & 0 & 0 & 0 & 0 & 0 & 0 & 0 & 0 & 0 \\ 0 & 1 & 0 & 0 & 0 & 0 & 0 & 0 & 0 & 0 \\ 0 & 2 & 0 & 0 & 0 & 0 & 0 & 0 & 0 & 0 \end{bmatrix}, \quad (3)$$

where the depth of T is 3. M_L is filled with an appropriate number based on the structure of the subtree. The 1st level of nodes in M_L has four and three children, respectively.

Fig. 11 shows the re-assignment results according to the propagation steps. The entire coverage area of R_E is first assigned to the 1st level of nodes in T according to A_{R_i} . Subsequently, the partial coverage areas of the robots corresponding to 1st level of nodes in T are assigned to the

2nd level of nodes in T according to A_{R_i} . For the 3rd and 4th levels of nodes, these processes are repeated. After the re-assignment process was completed, the coverage area of R_E was perfectly assigned to the remaining robots.

C. RESULTS OF THE BALANCED NODE ASSIGNMENT ACCORDING TO THE NUMBER OF ROBOTS

To verify the performance of the balanced node assignment, the mean of the balanced node assignment, named $MBAL_E$, is defined and computed as follows:

$$MBAL_E = \frac{1}{N_R - 1} \sum_{i \neq R_A}^{N_R} |(A_i^R - A_i^O - \frac{A_{R_A}}{N_R - 1})|, \quad (4)$$

where A_i^O and A_i^R are the coverage area of the i -th robot before and after the re-assignment process, respectively.

TABLE 2. MBL_E for several tests.

Environments	Totally recomputed for $N_R - 1$ [3]	Nearest neighbor-based method [34]	Proposed method
Map1, $N_R=3$	18.6	4.16	4.16
Map1, $N_R=5$	11.75	4.49	2.44
Map1, $N_R=10$	1.75	2.21	1.15
Map2, $N_R=3$	68.83	24.16	21.5
Map2, $N_R=5$	31.95	8.35	1.95
Map2, $N_R=10$	5.187	3.02	0.84

Table 2 represents $MBAL_E$ values of the three methods over several tests. The smaller result indicates more uniform allocation of the area of the excluded robot. It is clear from the results that the proposed method redistributes the coverage area of the excluded robot to the remaining robots most uniformly.

D. VARIATION OF THE INDIVIDUAL COVERAGE AREA BEFORE AND AFTER THE RE-ASSIGNMENT PROCESS

The variation in the individual coverage area before and after the re-assignment process is an important evaluation factor to determine how smoothly the individual coverage missions can be linked (meaning the seamless performance of the coverage task). In addition, the coverage mission can be effective after re-assignment.

The mean of this factor is $MVAR_E$ which is computed as follows:

$$MVAR_E = \frac{1}{N_R - 1} \sum_{i \neq R_A}^{N_R} \left(n \left(V_p^{i,O} - V_p^{i,R} \right) + n \left(V_p^{i,R} - V_p^{i,O} \right) \right), \quad (5)$$

where $V_p^{i,O}$ and $V_p^{i,R}$ are the nodes before and after the re-assignment process, respectively. $n(\cdot)$ represents the cardinality of a set. Since $A - B$ is the difference between the two sets, $n(V_p^{i,O} - V_p^{i,R})$ denotes the number of nodes taken from the child node of the i -th robot in T after the re-assignment. In addition, $n(V_p^{i,R} - V_p^{i,O})$ is the number

of additional nodes assigned from the parent node of the robot after re-assignment. $MVAR_E$ was computed for all experiments, as shown in Table 3.

TABLE 3. $MVAR_E$ over the several tests.

Environments	Totally recomputed for $N_R - 1$ [3]	Nearest neighbor-based method [34]	Proposed method
Map1, $N_R=3$	24.3	16	16
Map1, $N_R=5$	18.7	6.5	8.25
Map1, $N_R=10$	5.7111	0.55	1.67
Map2, $N_R=3$	53.83	10.5	20
Map2, $N_R=5$	38.8	5	10.75
Map2, $N_R=10$	11.5	0.889	2.33

If the result is small, each robot can achieve seamless coverage without significant changes in the coverage area. The proposed method reduces the change in the coverage area by at least 1.5 times and at most 5 times compared to the method of recalculating the entire area. However, the proposed method has better results in most cases than the nearest neighbor-based method. This is because the nearest neighbor-based method only makes a coverage change for the robot to the excluded robot. In addition, in the proposed method, all robots bear the burden equally to balance the amount of re-assignment of the coverage area, which increases the coverage variation before and after relocation.

E. ALGORITHM EXECUTION TIME COMPARISON

The last thing to note is the duration for which each method is performed. The PC used for algorithm execution time comparison was equipped with an AMD Ryzen Threadripper 3970X 32-core processor and 256GB of RAM. Three different methods were compared for different environments on the same PC. The first method (the totally recomputed method) takes longer on average than the other two methods because it recalculates the entire coverage area without using the initial coverage area assignment. The proposed and NN methods performed relatively quickly compared to the first method. However, the proposed method took slightly longer on average than the nearest neighbor-based method. This is because the proposed method is performed for all robots by propagation, whereas the nearest neighbor-based method is performed only for robots closest to the excluded robot. However, this time difference is not a significant problem considering the meaning of the re-assignment process that is not performed frequently.

V. DISCUSSION

In this study, if one robot in the coverage area of the robot team leaves the coverage mission owing to charging or breakdown, the proposed method is for the remaining robots to fill the robot coverage area. To evaluate the proposed method, three methods were evaluated according to three factors by varying the number of maps and robots in the

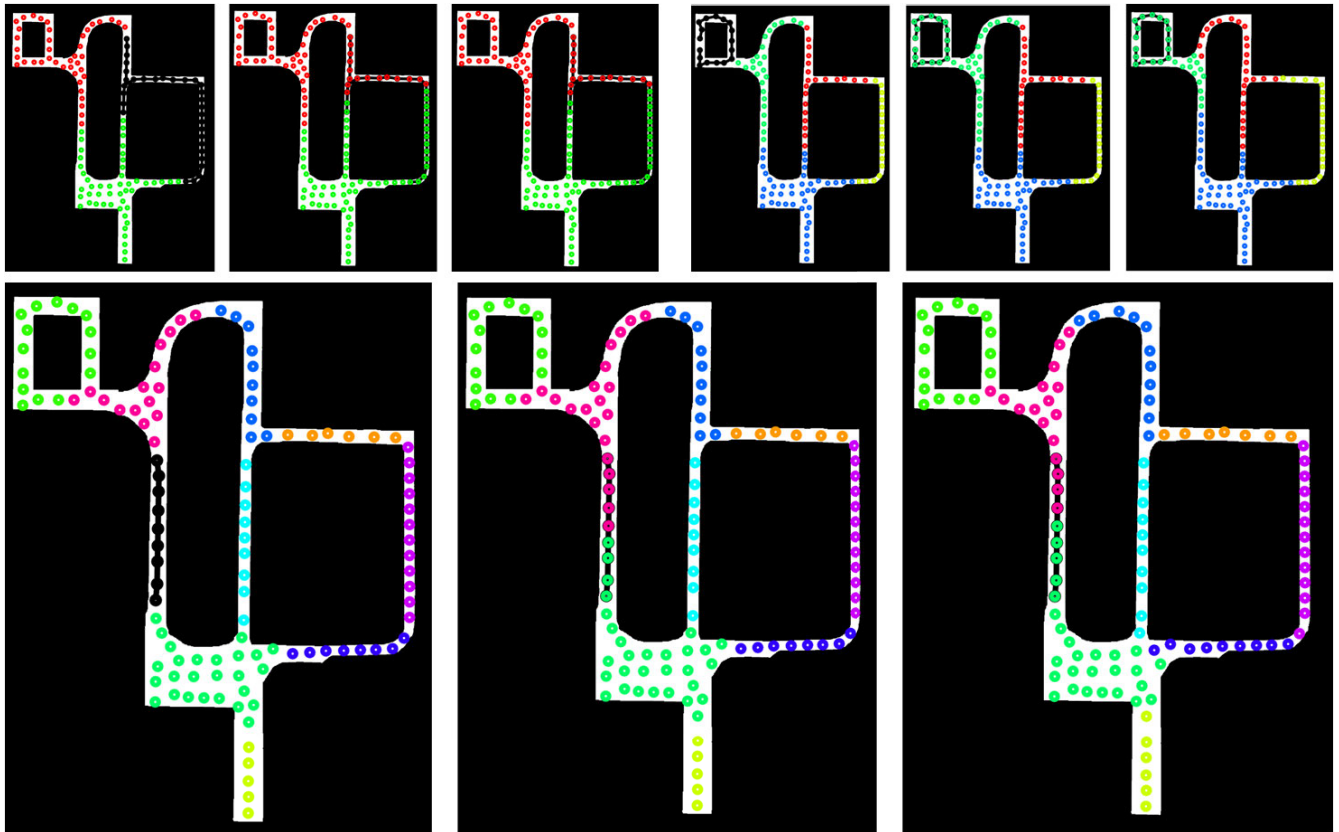


FIGURE 12. Comparison of coverage area re-assignment results in Map 1. This is the result of re-allocating the coverage area of Map1 for $N_R = 3, 5, 10$. The black nodes and paths shown in the first figure of each experiment represent the coverage path of the excluded robot. The second and third are the performance results of the nearest neighbor-based method and the proposed method, respectively. In the nearest neighbor method, only the coverage areas of robots adjacent to the excluded robot are changed. On the other hand, the proposed method equally divides the entire robot area through 'propagation'.

experiments. The performance of the proposed method is demonstrated by three factors: balanced re-assignment of the coverage area, variation of the individual coverage area before and after the re-assignment process, and overall computation time.

TABLE 4. Computation time comparison (SEC).

Environments	Totally recomputed method [3]	Nearest neighbor-based method [34]	Proposed method
Map1, $N_R=3$	0.59	0.093	0.09
Map1, $N_R=5$	0.55	0.093	0.10
Map1, $N_R=10$	0.61	0.09	0.10
Map2, $N_R=3$	0.40	0.08	0.12
Map2, $N_R=5$	0.38	0.10	0.12
Map2, $N_R=10$	0.55	0.09	0.12

First off, the proposed method showed lower values than the other methods in the evaluation of the balanced re-assignment of coverage areas. This implies that the coverage area is evenly delivered to the entire robot in the propagation scheme. This allows the robots to receive approximately the same amount of information and continuously perform

balanced coverage. In particular, as the number of robots increased, the value became very small, regardless of the environment. Owing to the nature of propagation, it can be observed that as the number of robots increases, the strength of the proposed method increases.

The second factor is the variation in the individual coverage area before and after the re-assignment process, which indicates change in the current coverage area. If this value is large, it means that there is a high degree of confusion in each robot's coverage mission performance after the re-assignment of the area. If the level of confusion is too high, the coverage mission area and paths will change significantly, which may result in robot-to-robot collisions while moving to the newly allocated area. In addition, if a robot is re-assigned a completely new area compared to its existing coverage area, it may take long time to complete the new coverage area. The proposed method yielded better results than the method that recalculates the total area. However, the proposed method showed a higher $MVAR_E$ than the method [32] because of its ability to change the entire robot coverage area. In addition, when calculating $MVAR_E$, it is divided by the total number of robots. However, in the method [32], because the number of robots that change the coverage area is the number of closest robots, $MVAR_E$ for effective robots changing the

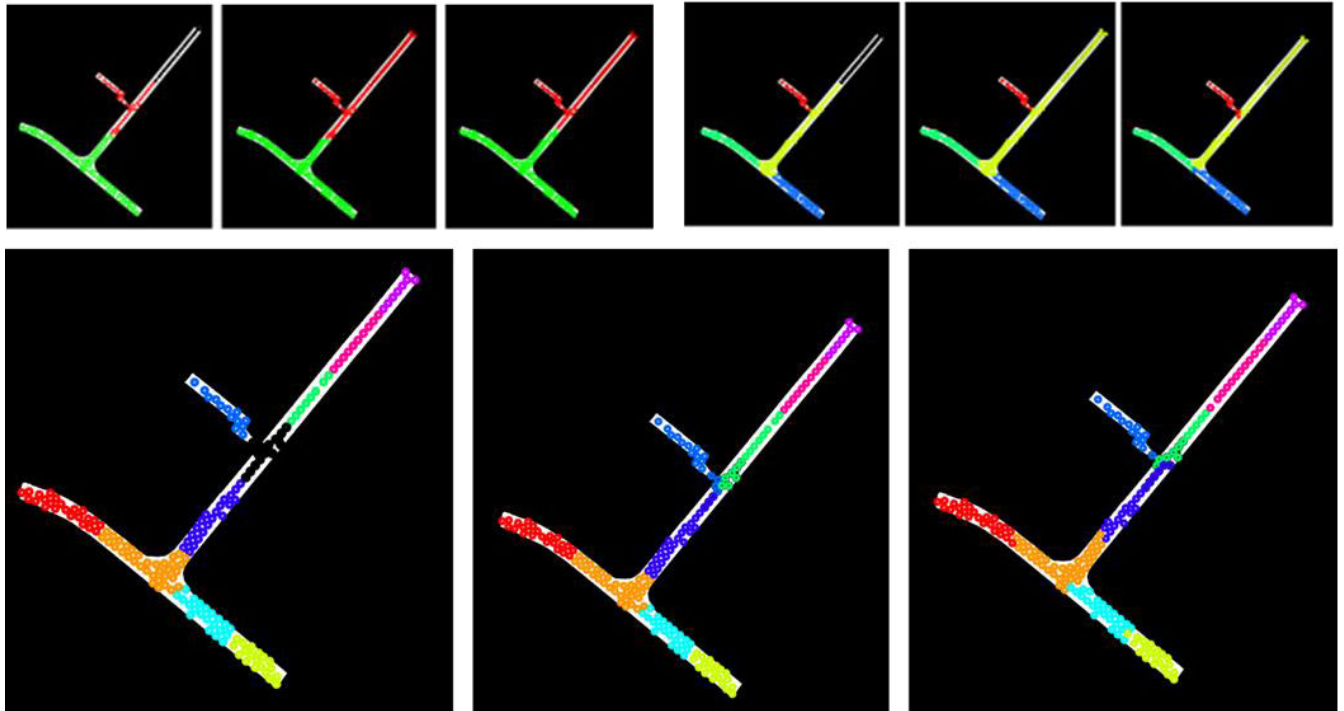


FIGURE 13. Comparison of Coverage area re-assignment results in Map 2. This is the result of re-allocating the coverage area of Map2 for $N_R = 3, 5, 10$. The black nodes and paths shown in the first figure of each experiment represent the coverage path of the excluded robot. The second and third are the performance results of the nearest neighbor based method and the proposed method, respectively. In the nearest neighbor method, only the coverage areas of robots adjacent to the excluded robot are changed. On the other hand, the proposed method equally divides the entire robot area through the propagation process.

coverage area increases as follows: (See data for effective robots in Table 5)

TABLE 5. $MVAR_E$ over several tests.

Environments	Nearest neighbor-based method	Nearest neighbor-based method (for effective robots)	Proposed method
Map1, $N_R=3$	16	16	16
Map1, $N_R=5$	6.5	8.67	8.25
Map1, $N_R=10$	0.55	5	1.67
Map2, $N_R=3$	10.5	21	20
Map2, $N_R=5$	5	20	10.75
Map2, $N_R=10$	0.889	4	2.33

The method [32] imposes a greater burden on each robot in contrast to the proposed method.

Lastly, in terms of the total computation time, the proposed method is on average faster than the full-area recalculation methods but slightly slower than the nearest-neighbor-based methods. As aforementioned, the method [32] is performed only on the closest robot from the excluded robot, but the proposed method is performed for all remaining robots. However, this lag is too small to be a major problem in real world systems. Moreover, based on the results of this study, a MRSS consisting of three mobile robots was configured and a long-term test was conducted without any issues arising from computational burden.

VI. CONCLUSION

In this study, the re-assignment of coverage was addressed in the multi-robot surveillance system. Any robot in a multi-robot surveillance team may be taken out of coverage missions due to battery charging or faulty issues. To overcome this problem, a strategy based on the propagation principle was proposed while minimizing the change in the coverage area for an individual robot and dividing the coverage area of the excluded robot into the remaining robots equally. For smooth propagation, a robot relational graph and tree structure have also been suggested. Coverage areas were differently assigned according to the depth of the tree, which resulted in balanced coverage area for all the remaining robots. The simulations were conducted using two experimental maps. The coverage area was uniformly re-allocated after the proposed method was applied. In addition, the proposed method has a short calculation time and enables seamless coverage even after re-allocation. In the future, probabilistic maps related to the importance rate, accident rate, and crowds in the coverage area will be considered.

REFERENCES

- [1] T. Alam and L. Bobadilla, "Multi-robot coverage and persistent monitoring in sensing-constrained environments," *Robotics*, vol. 9, no. 2, p. 47, Jun. 2020.
- [2] J. Scherer and B. Rinner, "Multi-robot patrolling with sensing idleness and data delay objectives," *J. Intell. Robot. Syst.*, vol. 99, nos. 3–4, pp. 949–967, Sep. 2020.

- [3] D. Noh, J. Choi, J. Choi, D. Byun, K. Youngjae, H.-R. Kim, S. Baek, S. Lee, and H. Myung, "MASS: Multi-agent scheduling system for intelligent surveillance," in *Proc. 19th Int. Conf. Ubiquitous Robots (UR)*, 2022, pp. 252–257.
- [4] S. H. Lee, "A new entrapment based invader capture strategy for multi-robot surveillance systems," in *Proc. Intell. Syst. Appl., Intell. Syst. Conf. (IntelliSys)*, 2022, pp. 318–327.
- [5] S. Lee, "A multi-robot balanced coverage path planning strategy for patrol missions," in *Proc. 21st Int. Conf. Control, Autom. Syst. (ICCAS)*, Oct. 2021, pp. 1567–1569.
- [6] X. Huang, M. Sun, H. Zhou, and S. Liu, "A multi-robot coverage path planning algorithm for the environment with multiple land cover types," *IEEE Access*, vol. 8, pp. 198101–198117, 2020.
- [7] R. Almadhoun, T. Taha, L. Seneviratne, and Y. Zweiri, "A survey on multi-robot coverage path planning for model reconstruction and mapping," *Social Netw. Appl. Sci.*, vol. 1, no. 8, pp. 1–24, Aug. 2019.
- [8] B. K. Patle, A. Pandey, D. R. K. Parhi, and A. Jagadeesh, "A review: On path planning strategies for navigation of mobile robot," *Defence Technol.*, vol. 15, pp. 582–606, Aug. 2019.
- [9] G. Sun, R. Zhou, B. Di, Z. Dong, and Y. Wang, "A novel cooperative path planning for multi-robot persistent coverage with obstacles and coverage period constraints," *Sensors*, vol. 19, no. 9, p. 1994, Apr. 2019.
- [10] F. Yasutomi, M. Yamada, and K. Tsukamoto, "Cleaning robot control," in *Proc. IEEE Int. Conf. Robot. Autom.*, Apr. 1988, pp. 1839–1841.
- [11] S. Koos, A. Cully, and J.-B. Mouret, "Fast damage recovery in robotics with the T-resilience algorithm," *Int. J. Robot. Res.*, vol. 32, no. 14, pp. 1700–1723, Dec. 2013.
- [12] S. Chakraborty, D. Elangovan, P. L. Govindarajan, M. F. Elnaggar, M. M. Alrashed, and S. Kamel, "A comprehensive review of path planning for agricultural ground robots," *Sustainability*, vol. 14, no. 15, p. 9156, Jul. 2022.
- [13] E. Galceran and M. Carreras, "A survey on coverage path planning for robotics," *Robot. Auton. Syst.*, vol. 61, no. 12, pp. 1258–1276, 2013.
- [14] K. R. Guruprasad and T. D. Ranjitha, "CPC algorithm: Exact area coverage by a mobile robot using approximate cellular decomposition," *Robotica*, vol. 39, no. 7, pp. 1141–1162, 2020.
- [15] B. Nasirian, M. Mehrandezh, and F. Janabi-Sharifi, "Efficient coverage path planning for mobile disinfecting robots using graph-based representation of environment," *Frontiers Robot. AI*, vol. 8, Mar. 2021, Art. no. 624333.
- [16] M. M. Rahman, K. Ishii, and N. Noguchi, "Optimum harvesting area of convex and concave polygon field for path planning of robot combine harvester," *Intell. Service Robot.*, vol. 12, no. 2, pp. 167–179, Apr. 2019.
- [17] X. Miao, H.-S. Lee, and B.-Y. Kang, "Multi-cleaning robots using cleaning distribution method based on map decomposition in large environments," *IEEE Access*, vol. 8, pp. 97873–97889, 2020.
- [18] C. S. Tan, R. Mohd-Mokhtar, and M. R. Arshad, "A comprehensive review of coverage path planning in robotics using classical and heuristic algorithms," *IEEE Access*, vol. 9, pp. 119310–119342, 2021.
- [19] D. Portugal and R. Rocha, "A survey on multi-robot patrolling algorithms," in *Proc. Doctoral Conf. Comput., Elect. Ind. Syst.*, 2011, pp. 139–146.
- [20] D. Portugal and R. Rocha, "MSP algorithm: Mmulti-robot patrolling based on territory allocation using balanced graph partitioning," in *Proc. ACM Symp. Appl. Comput.*, Mar. 2010, pp. 1271–1276.
- [21] Y. Elmaliach, N. Agmon, and G. A. Kaminka, "Multi-robot area patrol under frequency constraints," in *Proc. IEEE Int. Conf. Robot. Autom.*, Apr. 2007, pp. 385–390.
- [22] J. Chen, C. Du, Y. Zhang, P. Han, and W. Wei, "A clustering-based coverage path planning method for autonomous heterogeneous UAVs," *IEEE Trans. Intell. Transp. Syst.*, vol. 23, no. 12, pp. 25546–25556, Dec. 2022.
- [23] J. Chen, Y. Zhang, L. Wu, T. You, and X. Ning, "An adaptive clustering-based algorithm for automatic path planning of heterogeneous UAVs," *IEEE Trans. Intell. Transp. Syst.*, vol. 23, no. 9, pp. 16842–16853, Sep. 2022.
- [24] J. Chen, F. Ling, Y. Zhang, T. You, Y. Liu, and X. Du, "Coverage path planning of heterogeneous unmanned aerial vehicles based on ant colony system," *Swarm Evol. Comput.*, vol. 69, Mar. 2022, Art. no. 101005.
- [25] A. Gautam, V. S. Shekhawat, and S. Mohan, "A graph partitioning approach for fast exploration with multi-robot coordination," in *Proc. IEEE Int. Conf. Syst., Man Cybern. (SMC)*, Oct. 2019, pp. 459–465.
- [26] T. Alam, M. M. Rahman, P. Carrillo, L. Bobadilla, and B. Rapp, "Stochastic multi-robot patrolling with limited visibility," *J. Intell. Robot. Syst.*, vol. 97, no. 2, pp. 411–429, Feb. 2020.
- [27] N. Agmon, G. A. Kaminka, and S. Kraus, "Multi-robot adversarial patrolling: Facing a full-knowledge opponent," *J. Artif. Intell. Res.*, vol. 42, pp. 887–916, Dec. 2011.
- [28] D. Portugal and R. Rocha, "MSP algorithm: Multi-robot patrolling based on territory allocation using balanced graph partitioning," in *Proc. ACM Symp. Appl. Comput.*, Mar. 2010, pp. 1271–1276.
- [29] P. Fazli, A. Davoodi, and A. K. Mackworth, "Multi-robot repeated area coverage: Performance optimization under various visual ranges," in *Proc. 9th Conf. Comput. Robot. Vis.*, May 2012, pp. 298–305.
- [30] P. Fazli, A. Davoodi, and A. K. Mackworth, "Multi-robot repeated area coverage," *Auto. Robots*, vol. 34, no. 4, pp. 251–276, May 2013.
- [31] K. Saulnier, D. Saldana, A. Prorok, G. J. Pappas, and V. Kumar, "Resilient flocking for mobile robot teams," *IEEE Robot. Autom. Lett.*, vol. 2, no. 2, pp. 1039–1046, Apr. 2017.
- [32] J. Song and S. Gupta, "CARE: Cooperative autonomy for resilience and efficiency of robot teams for complete coverage of unknown environments under robot failures," *Auto. Robots*, vol. 44, nos. 3–4, pp. 647–671, Mar. 2020.
- [33] D. Monderer and L. S. Shapley, "Potential games," *Games Econ. Behavior*, vol. 14, no. 1, pp. 124–143, May 1996.
- [34] J. O'Rourke, *Art Gallery Theorems and Algorithms*. Oxford, U.K.: Oxford Univ. Press, 1987.
- [35] A. Savkin and H. Huang, "Proactive deployment of aerial drones for coverage over very uneven terrains: A version of the 3D art gallery problem," *Sensors*, vol. 19, no. 6, p. 1438, Mar. 2019.
- [36] A. Gautam, S. P. A. Ram, V. S. Shekhawat, and S. Mohan, "Balanced partitioning of workspace for efficient multi-robot coordination," in *Proc. IEEE Int. Conf. Robot. Biomimetics (ROBIO)*, Dec. 2017, pp. 104–109.
- [37] H.-Y. Lin and Y.-C. Huang, "Collaborative complete coverage and path planning for multi-robot exploration," *Sensors*, vol. 21, no. 11, p. 3709, May 2021.
- [38] L. Li, D. Shi, S. Jin, Y. Kang, C. Xue, X. Zhou, H. Liu, and X. Yu, "Complete coverage problem of multiple robots with different velocities," *Int. J. Adv. Robot. Syst.*, vol. 19, no. 2, Mar. 2022, Art. no. 172988062210916.
- [39] Z. Shen, P. Agrawal, J. P. Wilson, R. Harvey, and S. Gupta, "CPPNet: A coverage path planning network," in *Proc. IEEE/MTS OCEANS*, Sep. 2021, pp. 1–5.
- [40] T. Cabreira, L. Brisolara, and P. R. Ferreira Jr., "Survey on coverage path planning with unmanned aerial vehicles," *Drones*, vol. 3, no. 1, p. 4, Jan. 2019.
- [41] C. D. Franco and G. Buttazzo, "Coverage path planning for UAVs photogrammetry with energy and resolution constraints," *J. Intell. Robot. Syst.*, vol. 83, pp. 445–462, Sep. 2016.
- [42] W. Hess, D. Kohler, H. Rapp, and D. Andor, "Real-time loop closure in 2D LiDAR SLAM," in *Proc. IEEE Int. Conf. Robot. Autom. (ICRA)*, May 2016, pp. 1271–1278.



SEUNGHWAN LEE (Member, IEEE) received the B.S. degree in electronic engineering and computer science from Kyungpook National University, Daegu, South Korea, in 2008, and the M.S. and Ph.D. degrees in electrical engineering and computer science from Seoul National University, Seoul, South Korea, in 2010 and 2015, respectively. From 2015 to 2018, he was a Senior Researcher with the Samsung Electronics Mechatronics and Manufacturing Technology Center, Suwon, South Korea. Since 2018, he has been an Assistant Professor with the School of Electronic Engineering, Kumoh National Institute of Technology, Gumi, South Korea. His research interests include multi-robot SLAM, multi-robot coverage path planning, and human-like navigation.

• • •